RESEARCH ACTIVITIES X
Okazaki Institute for Integrative Bioscience

X-A Single-Molecule Physiology

A single molecule of protein (or RNA) enzyme acts as a machine which carries out a unique function in cellular activities. To elucidate the mechanisms of various molecular machines, we need to observe closely the behavior of individual molecules, because these machines, unlike man-made machines, operate stochastically and thus cannot be synchronized with each other. By attaching a tag that is huge compared to the size of a molecular machine, or a small tag such as a single fluorophore, we have been able to image the individual behaviors in real time under an optical microscope. Stepping rotation of the central subunit in a single molecule of F_1-ATPase has been videotaped, and now we can discuss its detailed mechanism. RNA polymerase has been shown to be a helical motor that rotates DNA during transcription. Myosin V and VI are also helical motors that move as a left- or right-handed spiral on the right-handed actin helix. Single-molecule physiology is an emerging field of science in which one closely watches individual, 'live' protein/RNA machines at work and examines their responses to external perturbations such as pulling and twisting. I personally believe that molecular machines operate by changing their conformations. Thus, detection of the conformational changes during function is our prime goal. Complementary use of huge and small tags is our major strategy towards this end.

http://www.k2.ims.ac.jp/

X-A-1 Catalysis and Rotation of F_1 Motor: Cleavage of ATP at the Catalytic Site Occurs in 1 ms before 40° Substep Rotation

SHIMABUKURO, Katsuya[1]; YASUDA, Ryohei[2]; MUNEYUKI, Eiro[1]; HARA, Kiyotaka Y.[3]; KINOSITA, Kazuhiko, Jr.; YOSHIDA, Masasuke[1,3]
([1]Tokyo Inst. Tech; [2]Cold Spring Harbor Laboratory; [3]ERATO)

[*Proc. Natl. Acad. Sci. U.S.A.* **100**, 14731–14736 (2003)]

F_1, a water-soluble portion of F_o F_1-ATP synthase, is an ATP hydrolysis-driven rotary motor. The central γ-subunit rotates in the $\alpha_3\beta_3$ cylinder by repeating the following four stages of rotation: ATP-binding dwell, rapid 80° substep rotation, interim dwell, and rapid 40° substep rotation. At least two 1-ms catalytic events occur in the interim dwell, but it is still unclear which steps in the ATPase cycle, except for ATP binding, correspond to these events. To discover which steps, we analyzed rotations of F_1 subcomplex ($\alpha_3\beta_3\gamma$) from thermophilic Bacillus PS3 under conditions where cleavage of ATP at the catalytic site is decelerated: hydrolysis of ATP by the catalytic-site mutant F_1 and hydrolysis of a slowly hydrolyzable substrate ATPγS (adenosine 5'-[γ-thio]triphosphate) by wild-type F_1. In both cases, interim dwells were extended as expected from bulk phase kinetics, confirming that cleavage of ATP takes place during the interim dwell. Furthermore, the results of ATPγS hydrolysis by the mutant F_1 ensure that cleavage of ATP most likely corresponds to one of the two 1-ms events and not some other faster undetected event. Thus, cleavage of ATP on F_1 occurs in 1 ms during the interim dwell, and we call this interim dwell catalytic dwell.

X-A-2 Mechanically Driven ATP Synthesis by F_1-ATPase

ITOH, Hiroyasu[1,2]; TAKAHASHI, Akira[1]; ADACHI, Kengo; NOJI, Hiroyuki[3]; YASUDA, Ryohei[4]; YOSHIDA, Masasuke[5]; KINOSITA, Kazuhiko, Jr.
([1]Hamamatsu Photonics; [2]CREST; [3]Univ. Tokyo; [4]Cold Spring Harbor Laboratory; [5]ERATO)

[*Nature* **427**, 465–468 (2004)]

ATP, the main biological energy currency, is synthesized from ADP and inorganic phosphate by ATP synthase in an energy-requiring reaction. The F_1 portion of ATP synthase, also known as F_1-ATPase, functions as a rotary molecular motor: *in vitro* its γ-subunit rotates against the surrounding $\alpha_3\beta_3$ subunits, hydrolysing ATP in three separate catalytic sites on the β-subunits. It is widely believed that reverse rotation of the γ-subunit, driven by proton flow through the associated F_o portion of ATP synthase, leads to ATP synthesis in biological systems. Here we present direct evidence for the chemical synthesis of ATP driven by mechanical energy. We attached a magnetic bead to the γ-subunit of isolated F_1 on a glass surface, and rotated the bead using electrical magnets. Rotation in the appropriate direction resulted in the appearance of ATP in the medium as detected by the luciferase–luciferin reaction. This shows that a vectorial force (torque) working at one particular point on a protein machine can influence a chemical reaction occurring in physically remote catalytic sites, driving the reaction far from equilibrium.

X-A-3 Chemomechanical Coupling in F_1-ATPase Revealed by Simultaneous Observation of Nucleotide Kinetics and Rotation

NISHIZAKA, Takayuki[1,2,6]; OIWA, Kazuhiro[1]; NOJI, Hiroyuki[3]; KIMURA, Shigeki[1]; MUNEYUKI, Eiro[4]; YOSHIDA, Masasuke[4,5]; KINOSITA, Kazuhiko, Jr.

([1]Kansai Adv. Res. Cent.; [2]PRESTO; [3]Univ. Tokyo; [4]Tokyo Inst. Tech; [5]ERATO; [6]Gakushuin Univ.)

[*Nat. Struct. Mol. Biol.* **11**, 142–148 (2004)]

F_1-ATPase is a rotary molecular motor in which unidirectional rotation of the central γ subunit is powered by ATP hydrolysis in three catalytic sites arranged 120° apart around γ. To study how hydrolysis reactions produce mechanical rotation, we observed rotation under an optical microscope to see which of the three sites bound and released a fluorescent ATP analog. Assuming that the analog mimics authentic ATP, the following scheme emerges: (i) in the ATP-waiting state, one site, dictated by the orientation of γ, is empty, whereas the other two bind a nucleotide; (ii) ATP binding to the empty site drives an ~80° rotation of γ; (iii) this triggers a reaction(s), hydrolysis and/or phosphate release, but not ADP release in the site that bound ATP one step earlier; (iv) completion of this reaction induces further ~40° rotation.

X-A-4 Unconstrained Steps of Myosin VI Appear Longest among Known Molecular Motors

ALI, Md. Yusuf[1]; HOMMA, Kazuaki[2]; IWANE, Atsuko H.[3]; ADACHI, Kengo; ITOH, Hiroyasu[4,5]; KINOSITA, Kazuhiko, Jr.; YANAGIDA, Toshio[3]; IKEBE, Mitsuo[2]

([1]Shahjalal Univ., Bangladesh; [2]Univ. Massachusetts Medical School, USA; [3]Osaka Univ.; [4]Hamamatsu Photonics; [5]CREST)

[*Biophys. J.* **86**, 3804–3810 (2004)]

Myosin VI is a two-headed molecular motor that moves along an actin filament in the direction opposite to most other myosins. Previously, a single myosin VI molecule has been shown to proceed with steps that are large compared to its neck size: either it walks by somehow extending its neck or one head slides along actin for a long distance before the other head lands. To inquire into these and other possible mechanism of motility, we suspended an actin filament between two plastic beads, and let a single myosin VI molecule carrying a bead duplex move along the actin. This configuration, unlike previous studies, allows unconstrained rotation of myosin VI around the right-handed double helix of actin. Myosin VI moved almost straight or as a right-handed spiral with a pitch of several micrometers, indicating that the molecule walks with strides slightly longer than the actin helical repeat of 36 nm. The large steps without much rotation suggest kinesin-type walking with extended and flexible necks, but how to move forward with flexible necks, even under a backward load, is not clear. As an answer, we propose that a conformational change in the lifted head would facilitate landing on a forward, rather than backward, site. This mechanism may underlie stepping of all two-headed molecular motors including kinesin and myosin V.

X-B Bioinorganic Chemistry of Heme-Based Sensor Proteins

Studies of heme-containing gas sensor proteins have revealed a novel function for heme, which acts as an active site for sensing the corresponding gas molecule of a physiological effector. Heme-based O_2, NO, and CO sensor proteins have now been found in which these gas molecules act as a signaling factor that regulates the functional activity of the sensor proteins. Our research interest focuses on the elucidation of structure-function relationships of CO sensor protein (CooA) and O_2 sensor protein (HemAT).

X-B-1 Activation Mechanisms of Transcriptinal Regulator CooA Revealed by Small-Angle X-Ray Scattering

AKIYAMA, Shuji[1]; FUJISAWA, Tetsuro[1]; ISHIMORI, Koichiro[2]; MORISHIMA, Isao[2]; AONO, Shigetoshi
([1]RIKEN Harima Inst./SPring 8; [2]Kyoto Univ.)

[*J. Mol. Biol.* **341**, 651–668 (2004)]

CooA, a heme-containing transcriptional activator, binds CO to the heme moiety and then undergoes a structural change that promotes the specific binding to the target DNA. To elucidate the activation mechanism coupled to CO binding, we investigated the CO-dependent structural transition of CooA with small-angle X-ray scattering (SAXS). In the absence of CO, the radius of gyration R_g and the second virial coefficient (A_2) were 25.3(±0.5) Å and –0.39(±0.25) × 10^{-4} ml mol g^{-2}, respectively. CO binding caused a slight increase in R_g (by 0.5 Å) and a marked decrease in A_2 (by 5.09 × 10^{-4} ml mol g^{-2}). The observed decrease in A_2 points to higher attractive interactions between CO-bound CooA molecules in solution compared with CO-free CooA. Although the minor alternation of R_g rules out changes in the overall structure, the marked change in the surface properties points to a CO-induced conformational transition. The experimental R_g and SAXS curves of the two states did not agree with the crystal structure of CO-free CooA. We thus simulated the solution structures of CooA based on the experimental data using rigid-body refinements as well as low-resolution model reconstructions. Both results demonstrate that the hinge region connecting the N-terminal heme domain and C-terminal DNA-binding domain is kinked in CO-free CooA, so that the two domains are positioned close to each other. The CO-dependent structural change observed by SAXS corresponds to a slight swing of the DNA-binding domains away from the heme domains coupled with their rotation by about 8 degrees around the axis of 2-fold symmetry.

X-B-2 Structure and Function of the CO-Sensor Protein CooA

AONO, Shigetoshi; YOSHIOKA, Shiro; INAGAKI, Sayaka

CooA is a heme-containing and CO-sensing transcriptional activator whose activity is regulated by CO, which is the first example of a transcriptional regulator containing a heme as a prosthetic group and of a heme protein in which CO plays a physiological role. A protoheme acts as a CO sensor in CooA. Mutagenesis and spectroscopic studies on CooA from *R. rubrum* (Rr-CooA) have revealed that the heme in Rr-CooA shows several unique features as described in the following: (1) The exchange of the axial ligand of the heme takes place during the change in the oxidation state of the heme iron. Cys^{75}, one of the axial ligands of the ferric heme, is replaced by His^{77} when the heme in CooA is reduced, and vice versa. (2) Hysteresis is observed in electrochemical redox titration, *i.e.*, the observed reduction and oxidation midpoint potentials are –320 mV and –260 mV, respectively. (3) Although the ferrous heme is 6-coordinate with two endogenous axial ligands, CO reacts with the ferrous heme to form the CO-bound heme under physiological conditions. Only CO-bound Rr-CooA is active as the transcriptional activator.

A CooA homologue from a thermophilic CO oxidizing bacterium, *C. hydrogenoformans*, (Ch-CooA) has also been studies. Ch-CooA shows different properties from Rr-CooA for the coordination structure and redox properties. Some information of what is essential for CooA function have been elucidated by comparing the properties between Ch-CooA and Rr-CooA.

X-B-3 Structure and Function of the Oxygen Sensing Signal Transducer Protein HemAT from *Bacillus subtilis*

AONO, Shigetoshi; YOSHIOKA, Shiro; KOBAYASHI, Katsuaki; YOSHIMURA, Hideaki

HemAT-Bs is a heme-containing signal transducer protein responsible for aerotaxis of *Bacillus subtilis*, where the heme acts as an oxygen sensor. We have characterized the recombinant HemAT-Bs to elucidate the mechanisms of oxygen-sensing and signal transduction by HemAT-Bs. HemAT-Bs shows similar uv/vis spectra to those of myoglobin (Mb). Site-directed mutagenesis reveals that His123 is the proximal ligand of the heme in HemAT-Bs.

Oxygen binding and dissociation rate constants are determined to be k_{on} = 32 μM^{-1} s^{-1} and k_{off} = 23 s^{-1}, respectively, revealing that HemAT-Bs has a moderate oxygen affinity similar to that of sperm whale Mb. The rate constant for autoxidation at 37 °C is 0.06 h^{-1}, which is also close to that of Mb. Although the electronic absorption spectra of HemAT-Bs are similar to those of Mb, HemAT-Bs shows some unique characteristics in its resonance Raman spectra. Oxygen-bound HemAT-Bs gives the ν(Fe–O_2) band at a noticeably low frequency (560 cm^{-1}), which suggests a unique hydrogen bonding between a distal amino acid residue and the proximal atom of the bound oxygen molecule. Deoxy HemAT-Bs gives the ν(Fe–His) band at a higher fre-

quency (225 cm^{-1}) than those of ordinary His-coordinated deoxy heme proteins.

HemAT-Bs consists of two domains, a N-terminal sensor domain and a C-terminal signaling domain. We have also prepared a truncated mutant consisting of the only N-terminal sensor domain. The heme environmental structure is perturbed by truncating the C-terminal domain. The resonance Raman spectroscopy reveals that a hydrogen bonding pattern toward the heme-bound oxygen is different from each other between wild-type and sensor domain mutant. The rate constant for autoxidation is 0.6 h^{-1} for the sensor domain mutant. The oxygen binding kinetics are also changed for the sensor domain mutant to be k_{on} = 69 μM^{-1} s^{-1} and k_{off} = 1.2 s^{-1}, indicating the binding affinity of oxygen increases in this mutant compared with wild-type HemAT-Bs.

X-C Electronic Structure and Reactivity of Active Sites of Metalloproteins

Metalloproteins are a class of biologically important macromolecules that have various functions such as oxygen transport, electron transfer, oxidation, and oxygenation. These diverse functions of metalloproteins have been thought to depend on the ligands from amino acid, coordination structures, and protein structures in immediate vicinity of metal ions. In this project, we are studying the relationship between the structures of the metal active sites and functions of metalloproteins.

X-C-1 A Salen Iron Complex as a Model for Non-Heme Iron Enzymes; Electronic Structure and Reactivity of the Two-Electron-Oxidized State

KURAHASHI, Takuya; KOBAYASHI, Yoshio[1]; FUJII, Hiroshi
([1]RIKEN)

High-valent iron-oxo species are proposed to be the key reactive intermediate in oxidation reactions catalyzed by both heme and non-heme iron enzymes. Although oxo-iron (IV) porphyrin π-cation radical and related model species have been extensively investigated in the field of heme chemistry, non-heme counterparts are not well understood. We employ the salen ligand as a non-heme iron model complex, and attempt to isolate a transient oxidizing intermediate. Herein, we describe spectroscopic properties of oxidizing intermediates and discuss the structure-reactivity relationship. We synthesize the salen iron complex **1** having bulky mesityl substituents to avoid an undesirable dimmerization. A low-temperature electrochemical oxidation generates one and two-electron oxidized forms of the complex **1**. Spectroscopic investigation by use of UV-Vis, CV, EPR, Mössbauer, and ESI mass spectroscopy indicates that the phenoxy radical iron complex is formed. The reactivity of the oxidized intermediate is also investigated. In contrast, the salen manganese complex **2** exhibits different spectroscopic behavior. In this study, the electronic structure of the oxidized intermediate from **2** is also discussed.

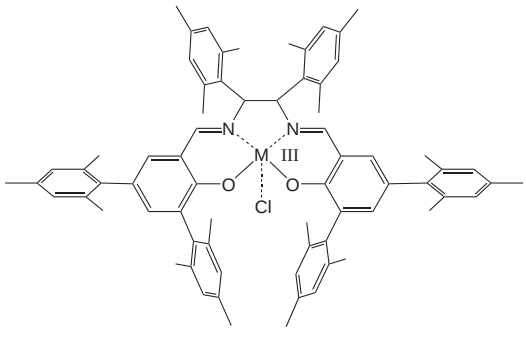

1 M = Fe; **2** M = Mn

Figure 1. Structure of Sterically Hindered Salen Complexes prepared in this study.

X-C-2 A Superoxo-Ferrous State in a Reduced Oxy-Ferrous Hemoprotein and Model Compounds

DAVYDOV, Roman[1]; SATTERLEE, James[2]; FUJII, Hiroshi; SAUER-MASARWA, Alexandra[3]; BUSCH, Daryle H.[3]; HOFFMAN, Brian M.[1]
([1]Northwestern Univ.; [2]Washington State Univ.; [3]Univ. Kansas)

[*J. Am. Chem. Soc.* **125**, 16340–16346 (2003)]

Cryoreduction of the $[FeO_2]^6$ (n = 6 is the number of electrons in 3d orbitals on Fe and π* orbitals on O_2) dioxygen-bound ferroheme through (irradiation at 77 K generates an $[FeO_2]^7$ reduced oxy-heme. Numerous investigations have examined $[FeO_2]^7$ centers that have been characterized as peroxo-ferric centers, denoted $[FeO_2]^7_{per}$, in which a ferriheme binds a dianionic peroxo-ligand. The generation of such an intermediate can be understood heuristically if the $[FeO_2]^6$ parent is viewed as a superoxo-ferric center and the injected electron localizes on the O–O moiety. We here report EPR/ENDOR experiments which show quite different properties for the $[FeO_2]^7$ centers produced by cryoreduction of monomeric oxy-hemoglobin (oxy-GMH3) from *Glycera dibranchiata*, which is unlike mammalian globins in having a leucine in place of the distal histidine, and of frozen aprotic solutions of oxy-ferrous octaethyl porphyrin and of the oxy-ferrous complex of the heme model, cyclidene. These $[FeO_2]^7$ centers are characterized as superoxo-ferrous centers, ($[FeO_2]^7_{sup}$), with nearly unit spin density localized on a superoxo moiety which is end-on coordinated to a low-spin ferrous ion. This assignment is based on their g tensors and ^{17}O hyperfine couplings, which are characteristic of the superoxide ion coordinated to a diamagnetic metal ion, and on the absence of detectable endor signals either from the in-plane ^{14}N ligands or from an exchangeable H-bond proton. Such a center would arise if the electron that adds to the $[FeO_2]^6$ superoxo-ferric parent localizes on the Fe ion, to make a superoxo-ferrous moiety. Upon annealing to T > 150 K the $[FeO_2]^7_{sup}$ species recruit a proton and converts to peroxo/hydroperoxo-ferric ($[FeO_2H]^7$) intermediates. These experiments suggest that the primary reduction product is $[FeO_2]^7_{sup}$, and that the internal redox transition to $[FeO_2]^7_{per}/[FeO_2H]^7$ states is driven at least in part by Hbonding/proton donation by the environment.

X-C-3 Synthesis and Characterization of Copper(I)-Nitrite Complexes as a Model for a Reaction Intermediate of Copper Nitrite Reductase

KUJIME, Masato; FUJII, Hiroshi

Cu-containing nitrite reductase (NiR) contains a pair of Cu, a type1 Cu ion and a type2 Cu ion, which catalyze the reduction of NO_2^- to NO. In the catalytic reduction, type 2 Cu site receives one electron from type 1 Cu site, and reduce Cu-bound NO_2^- ion to NO with addition of two protons. In this study, we synthesized Cu(I)-nitrite complexes with various tridentate ligands, $TACN^{iPr}Cu(NO_2)$ (**1**), $TIC^{iPr}Cu(NO_2)$ (**2**), $TPM^{iPr}Cu(NO_2)$ (**3**), and $TPM^{Me}Cu(NO_2)$ (**4**), as a model for a reaction intermediate of NiR. Reaction of **1** ~ **3** with acetic acid or trifuluoroacetic acid afforded Cu(II) species, which characterized by UV-Vis and ESR. NO gas generated in the reaction was trapped with Fe(II)-octaethylporphyrinate and detected as a NO-Heme complex by ESR. In addition, two equivalent of proton was required for quantitative generation of NO. Therefore, the complexes **1** ~ **3** produce NO upon addition of two protons and one-electron to the Cu-bound NO_2^-, similar to native NiR. The rate of NO evolution was accelerated by the use of trifuluoroacetic acid instead of acetic acid, suggesting that the rate-determining step is the protonation of Cu-bound NO_2^-.

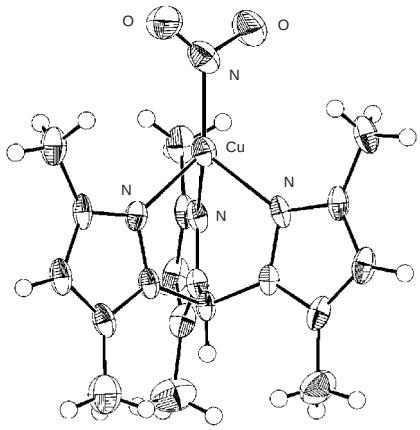

Figure 1. X-ray Crystal Structure of Copper(I)-Nitrite Complex.

X-D Molecular Mechanism of Heme Degradation and Oxygen Activation by Heme Oxygenase

Heme oxygenase (HO), an amphipathic microsomal protein, catalyzes the regiospecific oxidative degradation of iron protoporphyrinIX (heme) to biliverdinIXa, carbon monoxide, and iron in the presence of NADPH-cytochrome P-450 reductase, which functions as an electron donor. Heme oxygenase reaction is the biosynthesis processes of bile pigments and CO, which is a possible physiological messenger. Recent development in the bacterial expression of a soluble form of heme oxygenase has made it possible to prepare in the large quantities for structural studies. In this project, we are studying the molecular mechanism of heme degradation and the oxygen activation by heme oxygenase using various spectroscopic methods.

X-D-1 Kinetic Isotope Effects on the Rate-Limiting Step of Heme Oxygenase Catalysis Indicate Concerted Proton Transfer/Heme Hydroxylation

DAVYDOV, Roman[1]; MATSUI, Toshitaka[2]; FUJII, Hiroshi; IKEDA-SAITO, Masao[2]; HOFFMAN, Brian M.[1]
([1]Northwestern Univ; [2]Tohoku Univ.)

[*J. Am. Chem. Soc.* **125**, 16208–16209 (2003)]

Heme oxygenase (HO) catalyzes the O_2 and NADPH/cytochrome P450 reductase-dependent conversion of heme to biliverdin, free iron ion, and CO through a process in which the heme participates as both dioxygen-activating prosthetic group and substrate. We earlier confirmed that the first step of HO catalysis is a monooxygenation in which the addition of one electron and two protons to the HO oxy-ferroheme produces ferric-meso-hydroxyheme (**h**). Cryoreduction/EPR and ENDOR measurements further showed that hydroperoxo-ferri-HO converts directly to **h** in a single kinetic step without formation of a Compound I. We here report details of that rate-limiting step. One-electron 77 K cryoreduction of human oxy-HO and annealing at 200 K generates a structurally relaxed hydroperoxo-ferri-HO species, denoted **R**. We here report the cryoreduction/annealing experiments that directly measure solvent and secondary kinetic isotope effects (KIEs) of the rate-limiting **R** → **h** conversion, using enzyme prepared with meso-deuterated heme and in H_2O/D_2O buffers to measure the solvent KIE (solv-KIE), and the secondary KIE (sec-KIE) associated with the conversion. This approach is unique in that KIEs measured by monitoring the rate-limiting step are not susceptible to masking by KIEs of other processes, and these results represent the first direct measurement of the KIEs of product formation by a kinetically competent reaction intermediate in any dioxygen-activating heme enzyme. The observation of both solv-KIE(298) = 1.8 and sec-KIE(298) = 0.8 (inverse) indicates that the rate-limiting step for formation of h by HO is a concerted process: proton transfer to the hydroperoxo-ferri-heme through the distal-pocket H-bond network, likely from a carboxyl group acting as a general acid catalyst, occurring in synchrony with bond formation between the terminal hydroperoxo-oxygen atom and the α-meso carbon to form a tetrahedral hydroxylated-heme intermediate. Subsequent rearrangement and loss of H_2O then generates **h**.

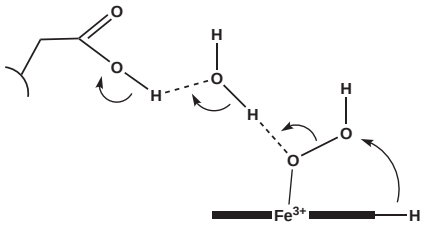

Figure 1. Mechanism of a proton transfer.

X-D-2 Essential Amino Acid Residues Controlling the Unique Regioselectivity of Heme Oxygenase in *Pseudomonas aeruginosa*

FUJII, Hiroshi; ZHANG, Xuhong[1]; YOSHIDA, Tadashi[1]

[*J. Am. Chem. Soc.* **126**, 4466–4467 (2004)]

Heme oxygenase (HO), an amphipathic microsomal protein, catalyzes the oxygen-dependent degradation of heme (iron-protoporphyrinIX) to -biliverdin, CO, and free iron ion. Interestingly, all of HO regiospecifically oxidize the α-meso position of the heme to form-biliverdin isomer while nonenzymatic heme degradation forms all four possible α-, β-, γ-, δ-biliverdin isomers at nearly identical yield. Recently, an interesting example has been found in HO (PigA) of the Gram-negative bacterium Pseudomonas aeruginosa, which does not produce α-biliverdin at all, but forms the mixture of β- and δ-biliverdins at a ratio of 3:7. While studying the mechanism of the unique regioselectivty of PigA, we found essential amino acid residues, Lys34, Lys132, and Phe189, controlling the unique regioselectivity of PigA. In this communication, we show that Lys34 and Lys132 are essential amino acid residues to hold the rotated heme in the active site of PigA via hydrogen-bonding interaction with the heme propionate and that Phe189 controls the product ratio of β- and δ-biliverdins *via* steric interaction with heme substituents. These interactions place the β- or δ-meso position of the heme at the oxidation site of PigA, leading to the unique regioselectivity.

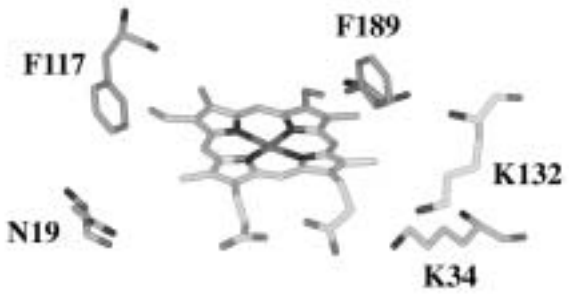

Figure 1. Active Site Structure of PigA-HO proposed in this study.

X-E Biomolecular Science

Elucidation of a structure-function relationship of metalloproteins and structural chemistry of amyloid are current subjects of this group. The primary technique used for the first project is the stationary and time-resolved resonance Raman spectroscopy excited by visible and UV lasers. Various model compounds of active site of enzymes are also examine with the same technique. IR-microscope dichroism analysis and AFM are the main techniques for the second project. The practical themes that we want to explore for the first project are (1) mechanism of oxygen activation by enzymes, (2) mechanism of active proton translocation and its coupling with electron transfer, (3) structural mechanism of signal sensing and transduction by heme-based sensor proteins, (4) higher order protein structures and their dynamics, and (5) reactions of biological NO. In category (1), we have examined a variety of terminal oxidases, cytochrome P450s, and peroxidases, and also treated their reaction intermediates by using the mixed flow transient Raman apparatus and the Raman/absorption simultaneous measurement device. For (2) the third-generation UV resonance Raman (UVRR) spectrometer was constructed and we are going to apply it to a giant protein like cytochrome *c* oxidase with M_r = 210,000. Recently, we succeeded in pursuing protein folding of apomyoglobin by combining UV time-resolved Raman and rapid mixing device. We also determined the carboxylic side chains of bovine cytochrome oxidase which undergo protonation/deprotonation changes and hydrogen-bonding status changes in response with electron transfers between metal centers or ligand dissociation from heme a_3. Currently, we focus our attention on detecting tyrosine radical for the P intermediate of terminal oxidases. In (3) we are interested in a mechanism of ligand recognition specific to CO, NO or O_2 and a communication pathway of the ligand binding information to the functional part of the protein. Several gas sensor heme proteins were extensively treated in this year. For (4) we developed a novel technique for UV resonance Raman measuremnts based on the combination of the first/second order dispersions of gratings and applied it successfully to 235-nm excited RR spectra of several proteins including mutant hemoglobins and myoglobins. Nowadays we can carry out time-resolved UVRR experiments with nanosecond resolution to discuss protein dynamics. With the system, we have succeeded in isolating the spectrum of tyrosinate in ferric Hb M Iwate, which was protonated in the ferrous state, and the deprotonated state of Tyr244 of bovine cytochrome *c* oxidase. The study is extended to a model of Tyr244, an imidazole-bound *para*-cresol coordinated to a metal ion, was synthesized and its UV resonance Raman was investigated. For (5) we purified soluble guanylate cyclase from bovine lung and observed its RR spectra in the presece of allosteric effectors. To further investigate it, we are developing an expression system of this protein. For the amyloid study, we examined FTIR spectra of β_2-microglobulin and its #11-21, K3, and K3-K7 peptides which form a core part of amyloid fibril.

X-E-1 Construction of a Square-Planar Hydroperoxo-Copper(II) Complex Inducing a Higher Catalytic Reactivity

FUJII, Tatsuya[1]; NAITO, Asako[1]; YAMAGUCHI, Syuhei[1]; WADA, Akira[1]; FUNAHASHI, Yasuhiro[1]; JITSUKAWA, Koichiro[1]; NAGATOMO, Shigenori; KITAGAWA, Teizo; MASUDA, Hideki[1]
([1]Nagoya Inst. Tech.)

[*Chem. Commun.* 2700–2701 (2003)]

A novel hydroperoxo-copper(II) complex with a square-planar geometry has been prepared, which has exhibited a higher selectivity and catalytic reactivity for dimethyl sulfide, in contrast to that with a trigonal-bipyramidal one.

X-E-2 Copper Hydroperoxo Species Activated by Hydrogen-Bonding Interaction with Its Distal Oxygen

YAMAGUCHI, Syuhei[1]; NAGATOMO, Shigenori; KITAGAWA, Teizo; FUNAHASHI, Yasuhiro[1]; OZAWA, Tomohiro[1]; JITSUKAWA, Koichiro[1]; MASUDA, Hideki[1]
([1]Nagoya Inst. Tech.)

[*Inorg. Chem.* **42**, 6968–6970 (2003)]

A novel copper(II)-OOH complex with functional ligand that can form a hydrogen bond with the distal oxygen of hydroperoxide has been designed and prepared as a structural/functional model of dopamine-hydroxylases, whose spectroscopic characterization and decomposition rates have indicated that the hydroperoxide is activated through the hydrogen-bonding interaction with the distal oxygen.

X-E-3 Thermal Stability and Absorption Spectroscopic Behavior of (μ-Peroxo)dicopper Complexes Regulated with Intramolecular Hydrogen Bonding Interactions

YAMAGUCHI, Syuhei[1]; WADA, Akira[1]; FUNAHASHI, Yasuhiro[1]; NAGATOMO, Shigenori; KITAGAWA, Teizo; JITSUKAWA, Koichiro[1]; MASUDA, Hideki[1]
([1]Nagoya Inst. Tech.)

[*Eur. J. Inorg. Chem.* **2003**, 4378–4386 (2003)]

In order to clarify the effect of hydrogen bonding on the stabilities of (μ-peroxo)dicopper complexes with a *trans*-1,2-peroxo form, novel copper complexes with intramolecular hydrogen bonding interaction sites have been synthesized, and their spectroscopic properties and thermal stabilities studied. The selected tripodal tetradentate ligands were tris(2-pyridylmethyl)amine (TPA) derivatives bearing pivalamido and amino groups at the

6-position of the pyridine ring in TPA, {[6-(pivalamido) pyrid-2-yl]methyl}bis(pyrid-2-ylmethyl)amine (MPPA) and [(6-aminopyrid-2-yl)methyl]bis(pyrid-2-ylmethyl) amine (MAPA). The single-crystal X-ray structure of a monomeric Cu^{II} complex with N_3^- namely [Cu(mppa) N_3]ClO_4 (**1a**), revealed an interligand hydrogen bonding interaction between the substituent NH group of MPPA and the azide nitrogen atom in the axial position. The Cu^I complexes of MPPA and MAPA were immediately oxygenated with dioxygen in acetone solution at –78 °C to give the μ-peroxo dinuclear copper(II) complexes $[\{Cu(mppa)\}_2(O_2)]^{2+}$ (**1b**) and $[\{Cu(mapa)\}_2(O_2)]^{2+}$ (**2b**). These complexes exhibited two kinds of characteristic absorption bands ($\pi^*_\sigma \rightarrow d_\sigma$, $\pi^*_v \rightarrow d_\sigma$) originating from the ligand-metal charge transfer (LMCT) of O_2^{2-} to Cu. Affected by the hydrogen bonding interaction, the π^*_d CT band shifted significantly to a higher energy region and the $\pi^*_v \rightarrow d_\sigma$ CT absorbance decreased due to stabilization of the π^* orbital and restriction of the Cu–O bond rotation. The thermal stabilities of the (μ-peroxo)dicopper(**II**) complexes were estimated from their decomposition rates which decreased in the order, **2b** $[\{Cu(tpa)\}_2(O_2)]^{2+}$ (**3b**) > **1b** >> $[\{Cu(6\text{-metpa})\}_2(O_2)]^{2+}$ (**4b**) {6-MeTPA = [(6-methylpyrid-2-yl)methyl] bis(pyrid-2-ylmethyl)amine}. The above findings indicate that the interligand hydrogen bonding interaction, although overcome to some extent by the adverse effect of the steric bulk of the NH group, is inclined to stabilize (μ-peroxo)dicopper(II) complexes.

X-E-4 CO Binding Study of Mouse Heme-Regulated eIF-2α Kinase: Kinetics and Resonance Raman Spectra

IGARASHI, Jotaro[1]; SATO, Akira[2]; KITAGAWA, Teizo; SAGAMI, Ikuko[3]; SHIMIZU, Toru[1]
([1]Tohoku Univ.; [2]GUAS; [3]Tohoku Univ. and Kyoto Prefectural Univ.)

[*Biochim. Biophys. Acta* **1650**, 99–104 (2003)]

Heme-regulated eukaryotic initiation factor (eIF)-2α kinase (HRI) regulates the synthesis of globin chains in reticulocytes with heme availability. In the present study, CO binding kinetics to the 6-coordinated Fe(II) heme of the amino-terminal domain of mouse HRI and resonance Raman spectra of the Fe(II)–CO complex are examined to probe the character of the heme environment. The CO association rate constant, k_{on}', and CO dissociation rate constant, k_{off}, were 0.0029 $\mu M^{-1}s^{-1}$ and 0.003 s^{-1}, respectively. These values are very slow compared with those of mouse neuroglobin and sperm whale myoglobin, while the koff value of HRI was close to those of the 6-coordinated hemoglobins from *Chlamydomonas* and barley (0.0022 and 0.0011 s^{-1}). The dissociation rate constant of an endogenous ligand, which occurs prior to CO association, was 18.3 s^{-1}, which was lower than those (197 and 47 s^{-1}) of the same 6-coordinate hemoglobins. Resonance Raman spectra suggest that the Fe–C–O adopts an almost linear and upright structure and that the bound CO interacts only weakly with nearby amino acid residues.

X-E-5 Resonance Raman Study on Synergistic Activation of Soluble Guanylate Cyclase by Imidazole, YC-1 and GTP

PAL, Biswajit; LI, Zhengqiang[1]; OHTA, Takehiro; TAKENAKA, Shigeo[2]; TSUYAMA, Shingo[2]; KITAGAWA, Teizo
([1]IMS and Jilin Univ.; [2]Osaka Prefecture Univ.)

[*J. Inorg. Biochem.* **98**, 824–832 (2004)]

Soluble guanylate cyclase (sGC), a physiological nitric oxide (NO) receptor, is a heme-containing protein and catalyzes the conversion of GTP to cyclic GMP. We found that 200 mM imidazole moderately activated sGC in the coexistence with 3-(5'-hydroxymethyl-2'-furyl)-1-benzylindazole (YC-1), although imidazole or YC-1 alone had little effect for activation. GTP facilitated this process. Resonance Raman spectra of imidazole complex of native sGC and CO-bound sGC (CO-sGC) have demonstrated that a simple heme adduct with imidazole at the sixth coordination position is not present for both sGC and CO-sGC below 200 mM of the imidazole concentration and that the Fe–CO stretching band (ν_{Fe-CO}) appears at 492 cm^{-1} in the presence of imidazole compared with 473 cm^{-1} in its absence. Both frequencies fall on the line of His-coordinated heme proteins in the ν_{Fe-CO} *vs* ν_{C-O} plot. However, it is stressed that the CO-heme of sGC becomes photo-inert in the presence of imidazole, suggesting the formation of five-coordinate CO-heme or of six-coordinate heme with a very weak trans ligand. These observations suggest that imidazole alters not only the polarity of heme pocket but also the coordination structure at the fifth coordination side presumably by perturbing the heme-protein interactions at propionic side chains. Despite the fact that the isolated sGC stays in the reduced state and is not oxidized by O_2, sGC under the high concentration of imidazole (1.2 M) yielded ν_4 at 1373 cm^{-1} even after its removal by gel-filtration, but addition of dithionite gave the strong ν_4 band at 1360 cm^{-1}. This indicated that imidazole caused autoxidation of sGC.

X-E-6 Heme Structures of Five Variants of Hemoglobin *M* Probed by Resonance Raman Spectroscopy

JIN, Yayoi[1]; NAGAI, Masako[1]; NAGAI, Yukifumi[1]; NAGATOMO, Shigenori; KITAGAWA, Teizo
([1]Kanazawa Univ.)

[*Biochemistry* **43**, 8517–8527 (2004)]

The α-abnormal Hb Ms show physiological properties different from the β-abnormal Hb Ms, that is, extremely low oxygen affinity of the normal subunit and extraordinary resistance to both enzymatic and chemical reduction of the abnormal met-subunit. To get insight into the contribution of heme structures to these differences among Hb Ms, we examined the 406.7-nm excited resonance Raman (RR) spectra of five Hb Ms in the frequency region from 1700 to 200 cm^{-1}. In the high-frequency region, profound differences between met-α

and met-β abnormal subunits were observed for the in-plane skeletal modes (the $\nu_{C=C}$, ν_{37}, ν_2, ν_{11} and ν_{38} bands), probably reflecting different distortions of heme structure caused by the out-of-plane displacement of the heme iron due to tyrosine coordination. Below 900 cm^{-1}, Hb M Iwate [α(F8)]His → Tyr], exhibited a distinct spectral pattern for the ν_{15}, γ_{11}, $\delta(C_bC_aC_b)_{2,4}$ and $\delta(C_bC_cC_d)_{6,7}$ compared to that of Hb M Boston [α(E7)] His → Tyr], although both heme irons are coordinated by Tyr. The β-abnormal Hb Ms, namely, Hb M Hyde Park [β(F8)]His → Tyr], Hb M Saskatoon [β(E7)]His → Tyr], and Hb M Milwaukee [β(E11)]Val → Glu], displayed RR band patterns similar to that of metHb A, but with some minor individual differences. The RR bands characteristic of the met-subunits of Hb Ms totally disappeared by chemical reduction and the ferrous heme of abnormal subunits was no more bonded with Tyr or Glu. They were bonded to the distal (E7) or proximal (F8) His, and this was confirmed by the presence of the ν_{Fe-His} mode at 215 cm^{-1} in the 441.6-nm excited RR spectra. A possible involvement of heme distortion in differences of reducibility of abnormal subunits and oxygen affinity of normal subunits is discussed.

X-E-7 Vibronic Coupling between Soret and Higher Energy Excited States in Iron(II) Porphyrins: Raman Excitation Profiles of A_{2g} Modes in the Soret Region

EGAWA, Tsuyoshi[1]; SUZUKI, Noriyuki[2]; DOKOH, Takashi[2]; HIGUCHI, Tsunehiko[2]; SHIMADA, Hideo[3]; KITAGAWA, Teizo; ISHIMURA, Yuzuru[3]
([1]IMS and Keio Univ.; [2]Univ. Tokyo; [3]Keio Univ.)

[*J. Phys. Chem. A* **108**, 568–577 (2004)]

Resonance Raman spectra were observed for heme proteins and iron(II) porphyrins including ferrous-CO and ferrous-isocyanide derivatives of cytochrome $P450_{cam}$, a synthetic iron(II) porphyrin complex having a thiolate axial ligand, ferrous-isocyanide derivative of myoglobin, and synthetic iron(II) porphyrin complexes having either an imidazole or a sulfide axial ligand. Among them, the former three were found to be a hyperporphyrin, giving red and blue Soret absorption bands, whereas others were normal porphyrins giving a single Soret band. When Raman scattering was excited within the Soret region, an anomalously polarized (ap) Raman line, which was assignable to the ν_{19} mode belonging to the A_{2g} species, was observed at 1537–86 cm^{-1} for all these compounds. Both the synthetic iron (II) porphyrins having the imidazole and sulfide ligands also showed another ap Raman line at 1230 cm^{-1}, which was assigned to ν_{26} of A_{2g} symmetry. Raman excitation profiles of the ν_{19} and ν_{26} modes showed a maximum that was displaced from the 0-0 component of the Soret or red Soret band toward higher frequencies by the frequency of the corresponding mode, indicating the 0-1 component. Although Raman lines of these modes were also observed upon excitation at the 0-0 component, they were significantly more intense at the 0-1 component. These results, together with nonadiabatic theories about vibronic contribution to Raman intensity, indicated the presence of vibronic coupling between the Soret (or red Soret) excited state and some other electronic excited state(s) located in the blue of the Soret band. The present study hence demonstrates that lower occupied orbitals other than those described in the ordinary four-orbital model and its extended form, which is applicable to the hyperporphyrins, contribute to the Soret (or red Soret) excited states.

X-E-8 Dioxygen Reactivity of Copper(I) Complexes with Tetradentate Tripodal Ligands Having Apliphatic Nitrogen Donors: Synthesis, Structures, and Properties of Peroxo and Superoxo Complexes

KOMIYAMA, Kazuya[1]; FURUTACHI, Hideki[1]; NAGATOMO, Shigenori; HASHIMOTO, Akifumi[1]; HAYASHI, Hideki[1]; FUJINAMI, Shuhei[1]; SUZUKI, Masatatsu[1]; KITAGAWA, Teizo
([1]Kanazawa Univ.)

[*Bull. Chem. Soc. Jpn.* **77**, 59–72 (2004)]

Oxygenation of copper(I) with tetradentate tripodal ligands (L) comprised of a tris(aminoethyl)amine (tren) skeleton having sterically bulky substituent(s) on the terminal nitrogens has been investigated, where L = tris(*N*-benzylaminoethyl)amine ($L^{H,Bn}$), tris(*N*-benzyl-*N*-methylaminoethyl)amine ($L^{Me,Bn}$), or tris(*N*,*N*-dimethylaminoethyl)amine ($L^{Me,Me}$). All the copper(I) complexes reacted with dioxygen at low temperatures to produce superoxocopper(II) and/or *trans*-(μ-1,2-peroxo)-dicopper(II) complexes depending on the steric bulkiness of the terminal nitrogens and the reaction conditions. The reaction of a copper(I) complex $[Cu(L^{H,Bn})]^+$ at –90 °C in acetone resulted in the formation of a superoxo complex $[Cu(L^{H,Bn})(O_2)]^+$ as a less stable species and a peroxo complex $[\{Cu(L^{H,Bn})\}_2(O_2)]^{2+}$ as a stable species. The structures of $[Cu(L^{H,Bn})]ClO_4$ and $[\{Cu(L^{H,Bn})\}_2(O_2)](BPh_4)_2\cdot 8(CH_3)_2CO$ were determined by X-ray crystallography. $[\{Cu(L^{H,Bn})\}_2(O_2)]^{2+}$ has a *trans*-(μ-1,2-peroxo)-dicopper(II) core with a trigonal bipyramidal structure. The O–O bond distance is 1.450(5) Å with an intermetallic Cu···Cu separation of 4.476(2) Å. The resonance Raman spectrum of $[\{Cu(L^{H,Bn})\}_2(O_2)]^{2+}$ measured at –90 °C in acetone-d6 showed a broad ν(O–O) band at 837–834 cm^{-1} (788 cm^{-1} for an ^{18}O labeled sample) and two ν(Cu–O) bands at 556 and 539 cm^{-1}, suggesting the presence of two peroxo species in solution. $[Cu(L^{Me,Bn})]^+$ also produced both superoxo and *trans*-μ-1,2-peroxo species, $[Cu(L^{Me,Bn})(O_2)]^+$ and $[\{Cu(L^{Me,Bn})\}_2(O_2)]^{2+}$. At a lower concentration of $[Cu(L^{Me,Bn})]^+$ (~0.24 mM) and higher dioxygen concentration ($P(O_2)$ = ~1 atm), the superoxo species is predominantly formed, whereas at a higher concentration of $[Cu(L^{Me,Bn})]^+$ (~1 mM) and lower dioxygen concentration ($P(O_2)$ = ~0.02 atm) the formation of the peroxo species is observed. The resonance Raman spectrum of $[Cu(L^{Me,Bn})(O_2)]^+$ (~1 mM) in acetone-d_6 at ~–95 °C exhibited a ν(O–O) band at 1120 cm^{-1} (1059 cm^{-1} for an ^{18}O labeled sample) and that of $[\{Cu(L^{Me,Bn})\}_2(O_2)]^{2+}$ (~3 mM) in acetone-d_6 at ~–90 °C showed two ν(O–O) bands at 812 and 797 cm^{-1} (767 and 753 cm^{-1} for an ^{18}O labeled sample),

respectively. A similar observation was also made for $[\{Cu(L^{Me,Me})\}_2(O_2)]^{2+}$. Relationships between the energies of the LMCT and *d–d* transitions and those of the ν(O–O) and ν(Cu–O) stretching vibrations and the steric constraints in the Cu(II)–(O_2^{2-})–Cu(II) core are discussed.

X-E-9 Dinuclear Copper-Dioxygen Intermediates Supported by Polyamine Ligands

TERAMAE, Shinichi[1]; OSAKO, Takao[2]; NAGATOMO, Shigenori; KITAGAWA, Teizo; FUKUZUMI, Shunichi[1]; ITOH, Shinobu[2]
([1]Osaka Univ.; [2]Osaka City Univ.)

[*J. Inorg. Biochem.* **98**, 746–757 (2004)]

Reactivity of the dicopper(I) and dicopper(II) complexes supported by novel polyamine ligands **L1** (1,11-bis(6-methylpyridin-2-yl)-2,6,10-triaza-2,6,10-tribenzylundecane) and **L2** (5-benzyl-1,9-bis(6-methylpyridin-2-yl)-2,8-bis(6-methylpyridin-2-ylmethyl)-2,5,8-triazanonane) towards O_2 and H_2O_2, respectively, has been investigated in order to shed light on the ligand effects on Cu_2/O_2 chemistry. The dicopper(I) complex of **L1** (**1a**) readily reacted with O_2 in a 2:1 ratio at a low temperature (–94 °C) in acetone to afford a mixture of (μ-η^2:η^2-peroxo)dicopper(II) and bis(μ-oxo)dicopper (III) complexes. The formation of these species has been confirmed by the electron spin resonance (ESR) silence of the solution as well as their characteristic absorption bands in the UV–visible region [max = 350 and 510 nm due to the peroxo complex and ~400 nm due to the bis(μ-oxo) complex] and the resonance Raman bands at 729 cm^{-1} [$\Delta\nu(^{16}O_2–^{18}O_2)$ = 38 cm^{-1}] due to the peroxo complex and at 611 and 571 cm^{-1} [$\Delta\nu(^{16}O_2–^{18}O_2)$ = 22 and 7 cm^{-1}, respectively] due to the bis(μ-oxo) complex. The peroxo and bis(μ-oxo) complexes were unstable even at the low temperature, leading to oxidative *N*-dealkylation at the ligand framework. The dicopper(I) complex of **L2** (**2a**) also reacted with O_2 to give (μ-hydroxo)dicopper(II) complex (**2b^{OH}**) as the product. In this case, however, no active oxygen intermediate was detected even at the low temperature (–94 °C). With respect to the copper(II) complexes, treatment of the (μ-hydroxo)dicopper(II) complex of **L1** (**1b^{OH}**) with an equimolar amount of H_2O_2 in acetone at –80 °C efficiently gave a (μ-1,1-hydroperoxo)dicopper(II) complex, the formation of which has been supported by its ESR-silence as well as UV–vis (370 and 650 nm) and resonance Raman spectra [881 cm^{-1}; $\Delta\nu(^{16}O_2–^{18}O_2)$ = 49 cm^{-1}]. The (μ-1,1-hydroperoxo)dicopper(II) intermediate of **L1** also decomposed slowly at the low temperature to give similar oxidative *N*-dealkylation products. Kinetic studies on the oxidative *N*-dealkylation reactions have been performed to provide insight into the reactivity of the active oxygen intermediates.

X-E-10 Structural Characterization of a Binuclear Center of a Cu-Containing NO Reductase Homologue from *Roseobacter denitrificans*: EPR and Resonance Raman Studies

MATSUDA, Yuji[1]; UCHIDA, Takeshi; HORI, Hiroshi[2]; KITAGAWA, Teizo; ARATA, Hiroyuki[1]
([1]Kyushu Univ.; [2]Osaka Univ.)

[*Biochim. Biophys. Acta* **1656**, 37–45 (2004)]

Aerobic phototrophic bacterium *Roseobacter denitrificans* has a nitric oxide reductase (NOR) homologue with cytochrome *c* oxidase (CcO) activity. It is composed of two subunits that are homologous with NorC and NorB, and contains heme *c*, heme *b*, and copper in a 1:2:1 stoichiometry. This enzyme has virtually no NOR activity. Electron paramagnetic resonance (EPR) spectra of the air-oxidized enzyme showed signals of two low-spin hemes at 15 K. The high-spin heme species having relatively low signal intensity indicated that major part of heme b_3 is EPR-silent due to an antiferromagnetic coupling to an adjacent Cu_B forming a Fe–Cu binuclear center. Resonance Raman (RR) spectrum of the oxidized enzyme suggested that heme b_3 is six-coordinate high-spin species and the other hemes are six-coordinate low-spin species. The RR spectrum of the reduced enzyme showed that all the ferrous hemes are six-coordinate low-spin species. ν(Fe–CO) and ν(C–O) stretching modes were observed at 523 and 1969 cm^{-1}, respectively, for CO-bound enzyme. In spite of the similarity to NOR in the primary structure, the frequency of ν(Fe–CO) mode is close to those of aa_3- and bo_3-type oxidases rather than that of NOR.

X-E-11 Model Complexes of the Active Site of Galactose Oxidase. Effects of the Metal Ion Binding Sites

TAKI, Masayasu[1]; HATTORI, Haruna[1]; OSAKO, Takao[1]; NAGATOMO, Shigenori; SHIRO, Motoo[2]; KITAGAWA, Teizo; ITOH, Shinobu[1]
([1]Osaka City Univ.; [2]Rigaku Agency)

[*Inorg. Chim. Acta* **357**, 3369–3381 (2004)]

Model compounds of the active site of galactose oxidase have been developed by using new cofactor model ligands, **L1H** (2-methylthio-4-*tert*-butyl-6-[{bis(pyridin-2-ylmethyl)amino}methyl]phenol) and **L2H** (2-methylthio-4-*tert*-butyl-6-[{bis(6-methylpyridin-2-ylmethyl)amino}methyl]phenol). Treatment of the ligands with copper(II) and zinc(II) perchlorate in the presence of triethylamine followed by anion exchange reaction with $NaPF_6$ or $NaBPh_4$ provided the corresponding copper(II) and zinc(II) complexes, the crystal structures of which have been determined by X-ray crystallographic analysis. All the copper(II) and zinc(II) complexes have been isolated as a dimeric form in which the phenolate oxygen of each ligand acts as the bridging ligand to form a rhombic $Mv(OAr)_2$ core (M = Cu or Zn). The dimeric complexes can be converted into the corresponding monomer complexes by the treatment with exogenous ligand such as acetate ion. The redox potential and the spectroscopic features of the monomer complexes have also been examined. Furthermore, the copper(II)- and zinc(II)-complexes of the phenoxyl radical species of the ligands have been generated in

situ by the oxidation of the phenolate complexes with $(NH_4)_2[Ce^{IV}(NO_3)_6]$ (CAN) in CH_3CN, and their spectroscopic features have been explored. The structures and physicochemical properties of the phenolate and phenoxyl radical complexes of **L1** and **L2** have been compared to those of the previously reported copper(II) and zinc(II) complexes of **L3** (2-methylthio-4-*tert*-butyl-6-[{bis(2-pyridin-2-ylethyl)amino}methyl]phenol) in order to get insights into the interaction between the metal ions and the organic cofactor moiety.

X-E-12 Refolding Processes of Cytochrome $P450_{cam}$ from Ferric and Ferrous Acid Forms to the Native Conformation

EGAWA, Tsuyoshi[1]; HISHIKI, Takako[2]; ICHIKAWA, Yusuke[2]; KANAMORI, Yasukazu[2]; SHIMADA, Hideo[2]; TAKAHASHI, Satoshi[3]; KITAGAWA, Teizo; ISHIMURA, Yuzuru[2]
([1]IMS and Keio Univ.; [2]Keio Univ.; [3]IMS and Osaka Univ.)

[*J. Biol. Chem.* **279**, 32008–32017 (2004)]

Changes in heme coordination state and protein conformation of cytochrome $P450_{cam}$ ($P450_{cam}$), a *b*-type heme protein, were investigated by employing pH jump experiments coupled with time-resolved optical absorption, fluorescence, circular dichroism, and resonance Raman techniques. We found a partially unfolded form (acid form) of ferric $P450_{cam}$ at pH 2.5, in which a Cys–heme coordination bond in the native conformation was ruptured. When the pH was raised to pH 7.5, the acid form refolded to the native conformation through a distinctive intermediate. Formations of similar acid and intermediate forms were also observed for ferrous $P450_{cam}$. Both the ferric and ferrous forms of the intermediate were found to have an unidentified axial ligand of the heme at the 6th coordination sphere, which is vacant in the high spin ferric and ferrous forms at the native conformation. For the ferrous form, it was also indicated that the 5th axial ligand is different from the native cysteinate. The folding intermediates identified in this study demonstrate occurrences of non-native coordination state of heme during the refolding processes of the large *b*-type heme protein, being akin to the well known folding intermediates of cytochromes *c*, in which *c*-type heme is covalently attached to a smaller protein.

X-E-13 Simultaneous Resonance Raman Detection of the Heme a_3-Fe-CO and Cu_B-CO Species in CO-Bound ba_3-Cytochrome *c* Oxidase from *Thermus thermophilus*

PINAKOULAKI, Eftychia[1]; OHTA, Takehiro; SOULIMANE, Tewfik[2]; KITAGAWA, Teizo; VAROTSIS, Constantinos[3]
([1]Univ. Crete; [2]Paul Scherrer Inst.; [3]IMS and Univ. Crete)

[*J. Biol. Chem.* **279**, 22791–22794 (2004)]

Understanding of the chemical nature of the dioxygen and nitric oxide moiety of ba_3-cytochrome *c* oxidase from *Thermus thermophilus* is crucial for elucidation of its physiological function. In the present work, direct resonance Raman (RR) observation of the Fe–C–O stretching and bending modes and the C–O stretching mode of the Cu_B–CO complex unambiguously establishes the vibrational characteristics of the heme-copper moiety in ba_3-oxidase. We assigned the bands at 507 and 568 cm^{-1} to the Fe–CO stretching and Fe–C–O bending modes, respectively. The frequencies of these modes in conjunction with the C–O mode at 1973 cm^{-1} showed, despite the extreme values of the Fe–CO and C–O stretching vibrations, the presence of the *a*-conformation in the catalytic center of the enzyme. These data, distinctly different from those observed for the caa_3-oxidase, are discussed in terms of the proposed coupling of the a-and b-conformations that occur in the binuclear center of heme-copper oxidases with enzymatic activity. The Cu_B–CO complex was identified by its ν(CO) at 2053 cm^{-1} and was strongly enhanced with 413.1 nm excitation indicating the presence of a metal-to-ligand charge transfer transition state near 410 nm. These findings provide, for the first time, RR vibrational information on the EPR silent Cu_B(I) that is located at the O_2 delivery channel and has been proposed to play a crucial role in both the catalytic and proton pumping mechanisms of heme-copper oxidases.

X-E-14 Detection of a Photostable Five-Coordinate Heme a_3-Fe-CO Species and Functional Implications of His384/α10 in CO-Bound ba_3-Cytochrome *c* Oxidase from *Thermus thermophilus*

OHTA, Takehiro; PINAKOULAKI, Eftychia[1]; SOULIMANE, Tewfik[2]; KITAGAWA, Teizo; VAROTSIS, Constantinos[1]
([1]Univ. Crete; [2]Paul Scherrer Inst.; [3]IMS and Univ. Crete)

[*J. Phys. Chem. B* **108**, 5389–5491 (2004)]

Resonance Raman (RR) spectra are reported for the fully reduced carbon monoxy derivative of ba_3-cytochrome *c* oxidase from *Thermus thermophilus*. The RR spectra show the formation of a photolabile six-coordinate heme-CO and a photostable five-coordinate heme Fe–CO species. The latter species is formed by the cleavage of the proximal heme Fe-His384 bond and is the first five-coordinate Fe–CO species detected in hemecopper oxidases. The frequency of the Fe–CO species observed at 526 cm^{-1} correlates with either the C–O stretching modes observed at 1967 or 1982 cm^{-1} and lie on the correlation line of ν(Fe–CO) *vs* ν(C–O) for all known five-coordinate heme Fe–CO complexes. The loss of intensity of the heme Fe-His384 mode observed at 193 cm^{-1} in the photostationary CO-bound spectra is attributed to the loss of the non-hydrogen bonded heme Fe–His384$\cdots$Gly359 conformer. Taken together, the data indicate that the environment of theruptured His384 that is a part of the *Q*-proton pathway and leads to the highly conserved among all hemecopper oxidases, H_2O pool, is disrupted upon CO binding to heme a_3.

X-E-15 Heme Environment in Aldoxime Dehydratase Involved in Carbon–Nitrogen Triple Bond Synthesis

OINUMA, Ken-Ichi[1]; OHTA, Takehiro; KONISHI, Kazunobu[1]; HASHIMOTO, Yoshiteru[1]; HIGASHIBATA, Hiroki[1]; KITAGAWA, Teizo; KOBAYASHI, Michihiko[1]
([1]Univ. Tsukuba)

[*FEBS Lett.* **568**, 44–48 (2004)]

Resonance Raman spectra have been measured to characterize the heme environment in aldoxime dehydratase (OxdA), a novel hemoprotein, which catalyzes the dehydration of aldoxime into nitrile. The spectra showed that the ferric heme in the enzyme is six-coordinate low spin, whereas the ferrous heme is five-coordinate high spin. We assign a prominent vibration that occurs at 226 cm^{-1} in the ferrous enzyme to the Fe-proximal histidine stretching vibration. In the CO-bound form of OxdA, the correlation between the Fe–CO stretching (512 cm^{-1}) and C–O stretching (1950 cm^{-1}) frequencies also supports our assignment of proximal histidine coordination.

X-E-16 Interactions of Soluble Guanylate Cyclase with Diatomics as Probed by Resonance Raman Spectroscopy

PAL, Biswajit; KITAGAWA, Teizo

[*J. Inorg. Biochem.* in press]

Soluble guanylate cyclase (sGC, EC 4.6.1.2) acts as a sensor for nitric oxide (NO), but is also activated by carbon monoxide in the presence of an allosteric modulator. Resonance Raman studies on the structure-function relations of sGC are reviewed with a focus on the CO-adduct in the presence and absence of allosteric modulator, YC-1, and substrate analogues. It is demonstrated that the sGC isolated from bovine lung contains one species with a five coordinate (5c) ferrous high-spin (HS) heme with the Fe–His stretching mode at 204 cm^{-1}, but its CO adduct yields two species with different conformations about the heme pocket with the Fe–CO stretching (ν_{Fe-CO}) mode at 473 and 489 cm^{-1}, both of which are His- and CO-coordinated 6c ferrous adducts. Addition of YC-1 to it changes their population and further addition of GTP yields one kind of 6c (ν_{Fe-CO} = 489 cm^{-1}) in addition to 5c CO-adduct (ν_{Fe-CO} = 521 cm^{-1}). Under this condition the enzymatic activity becomes nearly the same level as that of NO adduct. Addition of γ-S-GTP yields the same effect as GTP does but sGMP and GDP gives much less effects. Unexpectedly, ATP cancels the effects of GTP. The structural meaning of these spectroscopic observation is discussed in detail.

X-E-17 Resonance Raman Evidence for the Presence of Two Heme Pocket Conformations with Varied Activities in CO-Bound Bovine Soluble Guanylate Cyclase and Their Conversion

LI, Zhengqiang[1]; PAL, Biswajit; TAKENAKA, Shigeo[2]; TSUYAMA, Shingo[2]; KITAGAWA, Teizo
([1]IMS and Jilin Univ.; [2]Osaka Prefecture Univ.)

[*Biochemistry* in press]

It was noted previously that resonance Raman (RR) spectra of soluble guanylate cyclase (sGC) observed by five independent research groups were categorized into two types; sGC_1 and sGC_2 (Vogel, K. M., Hu, S. Z., Spiro, T. G., Dierks, E. A., Yu, A. E., and Burstyn, J. N., *J. Biol. Inorg. Chem.* **4**, 804–813 (1999)). We demonstrate here that the RR spectra of sGC isolated from bovine lung contains only sGC_2 but both species for CO-bound form (CO-sGC). The relative population of the two forms was changed from the initial CO-sGC_2 form dominant with the Fe–CO (ν_{Fe-CO}) and C–O stretching modes (ν_{CO}) at 472 and 1990 cm^{-1}, respectively, to the CO-sGC_1 form with ν_{Fe-CO} and ν_{CO} at 488 and 1973 cm^{-1} by adding a zenobiotic, YC-1. Further addition of a substrate, GTP, completed the change. GDP and cGMP had much less effects but a substrate analogue, GTP-γ-S was found to have the same effect as GTP. In contrast, ATP has the reverse effect, namely deleted the effect of YC-1 and GTP. In the coexistence of YC-1 and GTP, vinyl vibrations of heme are largely influenced and new CO-isotope sensitive bands were observed at 521, 488, 363, and 227 cm^{-1}. The 521 cm^{-1} band was assigned to the five-coordinate (5c) species from the model compound studies using ferrous iron-protoporphyrin IX in CTAB micelles. Distinctively from the 472 cm^{-1} species, both the 488-cm^{-1} and 521-cm^{-1} species were apparently unphotodissociable when an ordinary Raman spinning cell was used, meaning rapid recombination of photodissociated CO. On the basis of these observations, binding of YC-1 to the heme pocket is proposed.

X-E-18 SOUL in Mouse Eyes Is a Novel Hexameric Heme-Binding Protein with Characteristic Optical Absorption, Resonance Raman Spectral and Heme Binding Properties

SATO, Emiko[1]; SAGAMI, Ikuko[2]; UCHIDA, Takeshi; SATO, Akira[3]; KITAGAWA, Teizo; IGARASHI, Jotaro[1]; OLSON, John S.[4]; SHIMIZU, Toru[1]
([1]Tohoku Univ.; [2]Tohoku Univ. and Kyoto Prefectural Univ.; [3]GUAS; [4]Rice Univ.)

[*Biochemistry* in press]

SOUL is specifically expressed in the retina and pineal gland, and displays more than 40% sequence homology with p22HBP, a heme protein ubiquitously expressed in numerous tissues. SOUL was purified as a dimer in the absence of heme from the *E. coli* expression system, but displayed a hexameric structure upon heme binding. Heme-bound SOUL displayed optical absorption and resonance Raman spectra typical of 6-coordinate low-spin heme protein, with one heme per monomeric unit for both the Fe(III) and Fe(II) complexes. Spectral data additionally suggest that one of the axial ligands of the Fe(III) heme complex is His. Muta-

tion of His42 (the only His of SOUL) to Ala resulted in loss of heme binding, confirming that this residue is an axial ligand of SOUL. The K_d value of heme for SOUL was estimated as 4.8×10^{-9} M from the association and dissociation rate constants, suggesting high binding affinity. On the other hand, p22HBP was obtained as a monomer containing one heme per subunit, with a K_d value of 2.1×10^{-11} M. Spectra of heme-bound p22HBP were different from those of SOUL, but similar to those of heme-bound bovine serum albumin in which heme bound to a hydrophobic cavity with no specific axial ligand coordination. Therefore, the heme-binding properties and coordination structure of SOUL are distinct from those of p22HBP, despite high sequence homology. The physiological role of the new heme binding protein, SOUL, is further discussed in this report.

X-E-19 Quaternary Structures of Intermediately Ligated Human Hemoglobin A and Influences from Strong Allosteric Effectors; Resonance Raman Investigation

NAGATOMO, Shigenori; NAGAI, Masako[1]; MIZUTANI, Yasuhisa[2]; YONETANI, Takashi[3]; KITAGAWA, Teizo
([1]Kanazawa Univ.; [2]IMS and Kobe Univ.; [3]Univ. Pennsylvania)

[*Biophys. J.* submitted]

The Fe-histidine stretching (ν_{Fe-His}) frequency was determined for deoxy subunits of intermediately ligated human hemoglobin A in equilibrium and CO-photodissociated picosecond transient species in the presence and absence of strong allosteric effectors like inositol (hexakis)phosphate (IHP), bezafibrate (BZF) and 2,3-bisphosphoglycerate (BPG). The ν_{Fe-His} frequency of deoxyHb A was unaltered by the effectors. The T to R transition occurred around $m = 2 \sim 3$ in the absence of effectors but $m > 3.5$ in their presence, where m is the average number of ligands bound to Hb and was determined from the intensity of the ν_4 band measured in the same experiment. The α_1-β_2 subunit contacts revealed by UV resonance Raman spectra, which were distinctly different between the T and R states, remained unchanged by the effectors. This observation would solve the recent discrepancy that the strong effectors remove the cooperativity of oxygen binding in the low affinity limit whereas the ^{1}H NMR spectrum of fully ligated form exhibits the pattern of R state.

X-E-20 Oxygen Sensing Mechanism of HemAT from *Bacillus subtilis*: A Resonance Raman Spectroscopic Study

OHTA, Takehiro; YOSHIMURA, Hideaki; YOSHIOKA, Shiro; AONO, Shigetoshi; KITAGAWA, Teizo

[*J. Am. Chem. Soc.* submitted]

HemAT-*Bs* is a heme-based signal transducer protein responsible for aerotaxis of *Bacillus subtilis*, which detects oxygen and transmits the signal to regulatory proteins that control the direction of flagella rotation. CO and NO are also caught at the same position as O_2 but the signals would be differentiated. Binding of oxygen to the sensor domain of this protein is supposed to alter the protein conformation in the vicinity of heme, which is propagated to the signaling domain through the linker region in a way different from the other case in binding of other gases.

Specific sensing of O_2, CO, and NO might have been required for the aerophilic bacteria in the early times of the earth, when CO and NO were more abundant than O_2. In support of this idea our previous resonance Raman (RR) study of the oxygen bound form of HemAT-*Bs* has demonstrated that the Fe–O_2 stretching (ν_{Fe-O_2}) frequency (560 cm^{-1}) is noticeably lower than those of general oxygen bound hemoproteins, but similar to the frequencies observed for invertebrate, plant, and bacterial Hbs, suggesting that the bound oxygen is incorporated into a unique hydrogen bonding network in the distal environment. Here we present RR evidences for structural linkage between the distal heme pocket and the signaling domain by using the linker-lacking protein as well as the wild type and the Y70F and T95A mutants of full-length

X-E-21 The Interaction of Covalently Bound Heme with the Cytochrome *c* Maturation Protein CcmE

UCHIDA, Takeshi; STEVENS, Julie M.[1]; DALTROP, Oliver[1]; HARVAT, Edgar M.[1]; HONG, Lin[1]; FERGUSON, Stuart J.[1]; KITAGAWA, Teizo
([1]Univ. Oxford)

[*J. Biol. Chem.* submitted]

The heme chaperone CcmE is a novel protein that binds heme covalently *via* a histidine residue as part of its essential function in the process of cytochrome *c* biogenesis in many bacteria as well as plant mitochondria. In the continued absence of a structure of the holoform of CcmE, identification of the heme ligands is an important step in understanding the molecular function of this protein and the role of covalent heme binding to CcmE during the maturation of *c*-type cytochromes. In this work we present spectroscopic data that provide insight into the ligation of the heme iron in the soluble domain of CcmE from *E. coli*. Resonance Raman spectra demonstrated that one of the heme axial ligands is a histidine residue and the other is likely to be Tyr134. In addition, the properties of the heme resonances of the holo-protein compared with those of a form of CcmE with non-covalently bound heme provide evidence for the modification of one of the heme vinyl side chains by the protein, most likely the 2-vinyl group.

X-E-22 Role of Tyr288 at the Dioxygen Reduction Site of Cytochrome *bo* Studied by Stable Isotope Labeling and Site-Directed Mutagesis

UCHIDA, Takeshi; MOGI, Tatsushi[1]; NAKAMURA, Hiro[2]; KITAGAWA, Teizo
([1]Univ. Tokyo, Tokyo Inst. Tech. and ERATO(JST); [2]RIKEN Harima Inst. and Yokohama City Univ.)

[*J. Biol. Chem.* submitted]

To explore the role of a cross-link between side-chains of Tyr288 and His284 at the heme-copper binuclear center, we prepared cytochrome *bo* where D_4-, 1-^{13}C-, or 4-^{13}C-Tyr has been biosynthetically incorporated. Unexpectedly, the D_4-Tyr-labeled enzyme showed the large decrease in the ubiquinol-1 oxidase and CO-binding activities. Optical absorption and resonance Raman spectra identified the defect in the distal side of the heme-copper binuclear center. In the CO-bound D_4-Tyr-labeled enzyme, a large fraction of the $\nu_{(Fe–C)}$ mode was shifted from the normal 520 cm^{-1}-band to a broad band centered around 491 cm^{-1}, as found for the Y288F mutant. Our results suggest that the substitution of ring hydrogens of Tyr288 with deuteriums slows down the formation of the His-Tyr cross-link essential for the dioxygen reduction at the binuclear center.

X-E-23 Resonance Raman Characterization of the PAS-A Domain of the Nobel CO-Dependent Gene Regulatory Protein, NPAS2

UCHIDA, Takeshi; SATO, Emiko[1]; SATO, Akira[2]; SAGAMI, Ikuko[3]; SHIMIZU, Toru[1]; KITAGAWA, Teizo

([1]Tohoku Univ.; [2]GUAS; [3]Tohoku Univ. and Kyoto Prefectural Univ.)

[*J. Biol. Chem.* submitted]

Neuronal PAS domain protein 2, a newly discovered as a heme protein, is expressed in the mammalian forebrain and acts as a CO-dependent transcriptional activator. This protein consists of the N-terminal basic helix-loop-helix domain, and two heme-containing PAS domains (PAS-A and PAS-B). In this study we prepared the isolated PAS-A domain and its mutants, and measured resonance Raman spectra. The CO-bound form gave the $\nu_{Fe–CO}$ and $\nu_{C–O}$ bands at 497 and 1967 cm^{-1}, respectively, and the correlation plot between $\nu_{Fe–CO}$ and $\nu_{C–O}$ suggested that a neutral His is a trans ligand of CO. The ferric form is constituted of the dominant 6-coordinate low-spin species and minor 5- and 6-coordinate high-spin species. When its Raman spectrum was excited at 363.8 nm, an intense band assignable to the Fe^{3+}–S stretching was observed at 332 cm^{-1}, whereas it disappeared in the C170A mutant, suggesting that Cys170 is an axial ligand in the ferric state. The spectrum of the wild-type ferrous PAS-A domain shows a mixture of 5-coordinate high-spin and 6-coordinate low-spin hemes. In the H119A and H171A mutants, the 5-coordinate species increased, while no change was observed for the C170A mutant, which suggest that His119 and His171, not Cys170, are the axial ligands in the ferrous heme, and ligand replacement from Cys to His takes place upon heme reduction. The marker band ν_{11} of the reduced form, which is sensitive to the donor strength of the axial ligand, was shifted to a lower frequency than that of cytochrome c_3, suggesting the coordination of a deprotonated histidine. Taken together, the present results support a mechanism that CO binding to heme causes conformation change in the His171-Cys170 moiety, which leads to physiological signaling.

X-F Molecular Mechanism of Photosensory Protein Function, Excitation Energy Transfer and Electron Transfer in Biological Systems

We are interested in photochemistry, photophysics, photoenergy conversion and photosignal transduction in living orgamisms. Above all, the primary interest in our laboratory is the molecular mechanism of photosensory proteins including rhodopsin and photoactive yellow protein. Using theoretical/computational techniques, we study what happens in these photosensory proteins after light illumination and how these proteins convert light energy into conformational changes.

Excitation energy transfer is a significant process in biophysics. The light-harvesting antenna system in photosynthetic purple bacteria collects and transfers photoenergy efficiently by its unique mechanism. We study this mechanism theoretically.

The electron transfer in biological systems is mostly long-range electron transfer that occurs by the electron tunneling through the protein media. Using theoretical/computational methods, we calculate the electron tunneling current in the protein matrix and analyze how intraprotein electron transfer occurs.

X-F-1 Torsion Potential Works in Rhodopsin

YAMADA, Atsushi[1]; YAMATO, Takahisa[2]; KAKITANI, Toshiaki[1]; YAMAMOTO, Shigeyoshi[3]
([1]Nagoya Univ.; [2]IMS and Nagoya Univ.; [3]Chukyo Univ.)

[*Photochem. Photobiol.* **79**, 476–486 (2004)]

We investigate the role of protein environment of rhodopsin and the intramolecular interaction of the chromophore in the cis-trans photoisomerization of rhodopsin by means of a newly developed theoretical method. We theoretically produce modified rhodopsins in which a force field of arbitrarily chosen part of the chromophore or the binding pocket of rhodopsin is altered. We compare the equilibrium conformation of the chromophore and the energy stored in the chromophore of modified rhodopsins with those of native rhodopsins. This method is called site-specific force field switch (SFS). We show that this method is most successfully applied to the torsion potential of rhodopsin. Namely, by reducing the twisting force constant of the C11=C12 of 11-cis retinal chromophore of rhodopsin to zero, we found that the equilibrium value of the twisting angle of the C11=C12 bond is twisted in the negative direction down to about –80 degrees. The relaxation energy obtained by this change amounts to an order of 10 kcal/mol. In the case that the twisting force constant of the other double bond is reduced to zero, no such large twisting of the bond happens. From these results we conclude that a certain torsion potential is applied specifically to the C11=C12 bond of the chromophore in the ground state of rhodopsin. This torsion potential facilitates the bond-specific cis-trans photoisomerization of rhodopsin. This kind of the mechanism is consistent with our torsion model proposed by us more than a quarter of century ago. The origin of the torsion potential is analyzed in detail on the basis of the chromophore structure and protein conformation, by applying the SFS method extensively.

X-F-2 Role of Protein in the Primary Step of the Photoreaction of Yellow Protein

YAMADA, Atsushi[1]; ISHIKURA, Takakazu[1]; YAMATO, Takahisa[2]
([1]Nagoya Univ.; [2]IMS and Nagoya Univ.)

[*Proteins: Struct., Funct., Genet.* **55**, 1063–1069 (2004)]

We show the unexpectedly important role of the protein environment in the primary step of the photoreaction of the yellow protein after light illumination. The driving force of the *trans*-to-*cis* isomerization reaction was analyzed by a computational method. The force was separated into two different components: the term due to the protein-chromophore interaction and the intrinsic term of the chromophore itself. As a result, we found that the contribution from the interaction term was much greater than that coming from the intrinsic term. This accounts for the efficiency of the isomerization reaction in the protein environment in contrast to that in solution environments. We then analyzed the relaxation process of the chromophore on the excited-state energy surface and compared the process in the protein environment and that in a vacuum. Based on this analysis, we found that the bond-selectivity of the isomerization reaction also comes from the interaction between the chromophore and the protein environment.

X-F-3 Direct Measure of Functional Importance Visualized Atom-by-Atom for Photoactive Yellow Protein: Application to Photoisomerization Reaction

YAMADA, Atsushi[1]; ISHIKURA, Takakazu[1]; YAMATO, Takahisa[2]
([1]Nagoya Univ.; [2]IMS and Nagoya Univ.)

[*Proteins: Struct., Funct., Genet.* **55**, 1070–1077 (2004)]

Photoreceptor proteins serve as efficient nanomachines for the photoenergy conversion and the photosignal transduction of living organisms. For instance, the photoactive yellow protein derived from a halophilic bacterium has the *p*-coumaric acid chromophore, which undergoes an ultrafast photoisomerization reaction after light illumination. To understand the structure-function

relationship at the atomic level, we used a computational method to find *functionally important atoms* for the photoisomerization reaction of the photoactive yellow protein. In the present study, a "direct" measure of the functional significance was quantitatively evaluated for each atom by calculating the *partial atomic driving force* for the photoisomerization reaction. As a result, we revealed the reaction mechanism in which the specific role of each functionally important atom has been well characterized in a systematic manner. In addition, we observed that this mechanism is strongly conserved during the thermal fluctuation of the photoactive yellow protein.